ADVANCED FUNCTIONAL MATERIALS
www.afm-journal.de

Materials Views
www.MaterialsViews.com

Device Physics of White Polymer Light-Emitting Diodes

*Herman T. Nicolai, André Hof, and Paul W. M. Blom**

The charge transport and recombination in white-emitting polymer light-emitting diodes (PLEDs) are studied. The PLED investigated has a single emissive layer consisting of a copolymer in which a green and red dye are incorporated in a blue backbone. From single-carrier devices the effect of the green- and red-emitting dyes on the hole and electron transport is determined. The red dye acts as a deep electron trap thereby strongly reducing the electron transport. By incorporating trap-assisted recombination for the red emission and bimolecular Langevin recombination for the blue emission, the current and light output of the white PLED can be consistently described. The color shift of single-layer white-emitting PLEDs can be explained by the different voltage dependencies of trap-assisted and bimolecular recombination.

1. Introduction

Since the first report of an efficient organic light-emitting diode (OLED) by the Eastman Kodak group more than two decades ago,[1] the research field has progressed rapidly. OLEDs based on small molecules are nowadays widely used as pixels in mobile phone displays and prototypes of televisions employing OLEDs have been presented by several display manufacturers. The progress of polymer light-emitting diodes (PLEDs) is lagging behind, which can be understood from the different techniques used for the fabrication. In small-molecule-based OLEDs, the active layers are generally deposited by thermal evaporation. With this technique it is relatively straightforward to fabricate multilayer devices so that for all the processes that govern the device operation a separate layer can be used, which is individually optimized for that specific task. Polymers, on the other hand, are generally deposited using technologies based on solution processing, such as spin-coating or printing. Consequently it is more difficult to manufacture polymeric multilayer devices and PLEDs have not been able to match the efficiencies of small molecule OLEDs.

Thermal evaporation, however, requires relative expensive vacuum technology while solution processing holds the promise of cost efficient fabrication of large area devices. Solution-processed PLEDs may therefore hold a competitive edge over small molecule OLEDs for large area applications, such as lighting. The latter requires a broad emission over the full visible spectrum, which can be achieved in a number of ways. One approach is the fabrication of multilayered devices, where each layer emits light with a specific color so that the combined output is perceived as white.[2–4] As mentioned above, multilayer devices are difficult to process from solution due to the required solvent incompatibilities, which negates the advantage of simple and low-cost solution processed fabrication. Another approach is to use a blend of materials each emitting in a different color.[5–9] This approach requires absolute control over the morphology and suffers from phase segregation. An attractive way to avoid these complications is the use of a copolymer, in which red and green dyes are incorporated into a blue backbone.[10–13] In such a copolymer a small concentration of narrow bandgap dyes are copolymerized in a wide bandgap host polymer. The current is then carried by the polymer backbone and excitons formed on the backbone may transfer to the dyes, yielding simultaneous emission from the backbone and from the dye. Additionally, due to the smaller bandgap of the dyes, they may act as charge traps for the charge transport through the wide bandgap backbone and promote direct recombination on the dyes. As a result, in practice only a small concentration (<<1%) of dyes is required to obtain white light emission. By adjusting the dye concentrations, the color coordinate of the emission may be tuned.[14,15] The main advantage of using a white-emitting copolymer is that white light emission can be obtained using only one emissive layer that can be spin-coated or printed. This layer is then responsible for the injection of charges, the transport, and recombination. However, the fact that all these processes, and the emission of several colors, take place in a single-layer also severely complicates the understanding of the device operation.

An apparently inherent issue of single-layer white PLEDs is the color shift. It is usually observed that the emission spectrum exhibits a voltage dependence, ranging from red-white towards a blue-white with increasing bias.[5,8,9,16,17] Such a color shift is undesired since it makes PLEDs less suitable for dimmable lighting. The color shift of white PLEDs has been explained both by a saturation of the dyes[18,19] as well as by a shift of the recombination zone.[20] Gather et al. showed that the color shift in a single-layer white-emitting OLED can be explained by charge trapping and recombination on the dye.[21] In that work, the relative contributions from blue and red could be described by a simple model taking into account the trapping rate on the red dye.

H. T. Nicolai, Dr. A. J. Hof, Prof. P. W. M. Blom
Molecular Electronics, Zernike Institute for Advanced Materials
University of Groningen
Nijenborgh 4, NL-9747 AG Groningen, the Netherlands
E-mail: p.w.m.blom@rug.nl
Prof. P. W. M. Blom
Holst Centre, High Tech Campus 31
NL-5605 KN Eindhoven, the Netherlands

DOI: 10.1002/adfm.201102699

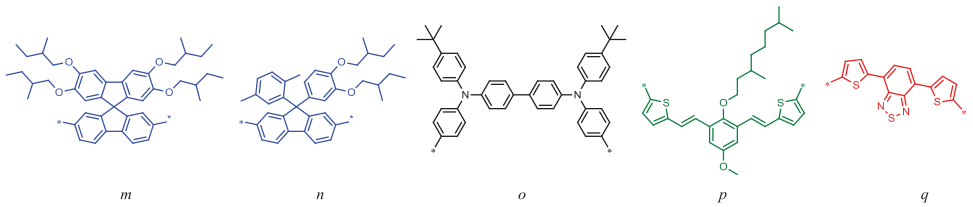

Figure 1. The structure of the polymers investigated. The components *p* and *q* are the green and red dyes, respectively. The composition of the blue polymer (B) is $m = 50\%$, $n = 40\%$, $o = 10\%$, $p = 0\%$, $q = 0\%$. For the blue-green copolymer (BG): $m = 50\%$, $n = 39.90\%$, $o = 0\%$, $p = 0.1\%$, $q = 0\%$ and for the white-emitting copolymer (BGR): $m = 50\%$, $n = 39.88\%$, $o = 10\%$, $p = 0.1\%$, $q = 0.02\%$.

The bimolecular recombination in PLEDs is shown to be limited by the diffusion of free electrons and holes toward each other in their mutual Coulomb field, which is described by the Langevin relation[22–24]

$$R_{\mathrm{Lan}} = \frac{q}{\varepsilon}\left(\mu_{\mathrm{e}} + \mu_{\mathrm{h}}\right)\left(np - n_{\mathrm{i}}^2\right) \tag{1}$$

with q the elementary charge, ε the dielectric constant, μ_{e} and μ_{h} the electron and hole mobilities, n and p the free electron and hole densities, and n_{i} the intrinsic carrier concentration. Whereas the hole transport in semiconducting polymers is generally observed to be trap-free, the electron transport is often found to be reduced by traps. As a result, a substantial part of the electron concentration is therefore localized in traps and does not contribute to the electron transport.[25–27] It has recently been demonstrated that an additional recombination process involving these trapped electrons constitutes a significant loss mechanism in PLEDs.[28] Recombination involving trapped carriers is described by the Shockley–Read–Hall (SRH) formalism[29,30]

$$R_{\mathrm{SRH}} = \frac{C_{\mathrm{n}} C_{\mathrm{p}} N_{\mathrm{t}}}{C_{\mathrm{n}}\left(n + n_1\right) + C_{\mathrm{p}}\left(p + p_1\right)}\left(np - n_{\mathrm{i}}^2\right) \tag{2}$$

with C_{n} and C_{p} the capture coefficients for electrons and holes, respectively, N_{t} the density of electron traps, and n_1 and p_1 the electron and hole densities in the case that the Fermi level coincides with the trap level. The most prominent difference between the Langevin and SRH mechanism is the different dependence on the charge carrier densities and consequently they exhibit a different voltage dependence in PLEDs.[28]

In a conventional PLED based on poly(*p*-phenylene vinylene) (PPV), the trap-assisted recombination is non-radiative and therefore constitutes a loss mechanism. It was shown that SRH recombination competes with Langevin recombination and that SRH recombination is dominant over Langevin recombination at low bias.[28] However, due to the different voltage dependence Langevin recombination eventually surpasses SRH recombination. Furthermore, it has been demonstrated that the current ideality factor of the diffusion regime is a measure for the strength of trap-assisted recombination, with an ideality factor of 2 indicating that trap-assisted recombination is dominant and an ideality factor of unity that Langevin recombination is dominant.[31,32] The measurement of the luminance ideality factor in conventional PLEDs revealed that the light emission originates from Langevin recombination, as expected. However, the luminance ideality factor of white PLEDs revealed different ideality factors for blue and red light. While the blue emission exhibits an ideality factor of unity (indicating Langevin recombination), the luminance ideality factor of the red emission amounts to 2, demonstrating that the red emission originates from trap-assisted recombination.[32]

In this study we apply a numerical device model[33] to describe the device operation of a single-layer white-emitting PLED. The device model solves Poisson's equation and the continuity equations using an iterative scheme and includes both drift and diffusion of charge carriers, the effect of charge traps,[26,27] and a mobility that depends on both electric field and the charge carrier density.[34] Both Langevin and SRH recombination are included. The mobility is described in the form of the extended Gaussian disorder model (EGDM), which is based on hopping in a Gaussian density of states (DOS).[35] In this formalism the mobility is described by three parameters: the site spacing a, the width of the Gaussian DOS σ, and the mobility in the limit of zero field, zero carrier density, and infinite temperature μ_0^*. In addition to the mobility parameters, the parameters describing the trap states are essential constituents of the device simulation because they determine the strength of the trap-assisted recombination. The large number of relevant parameters renders it a great challenge to achieve a quantitative description of the device operation.

In order to disentangle the various processes we investigate a set of three polymers (Merck KGaA) that contain an incremental number of dyes incorporated in the blue backbone: the blue backbone polymer (B), the backbone polymer with a green dye (BG), and the white-emitting polymer with both a green and red dye (BGR).[36,37] The structure of the white-emitting copolymer BGR is shown in **Figure 1**. The concentration of the green dye in the BGR and BG polymer is 0.1%, while the concentration of the red dye in the BGR polymer is 0.02%. The fact that the dyes are incorporated in a systematic way enables us to stepwise unravel the device operation of the white-emitting PLED.

2. Results

Figure 2 shows the photoluminescence (PL) and electroluminescence (EL) spectra of the three polymers investigated. Despite the low concentration of the green and red dye, a clear emission from the green dye can be observed upon the excitation of the blue backbone, demonstrating the energy transfer from the backbone to the dyes. Anni et al. have shown that the energy transfer is intermolecular and that energy transfer occurs from

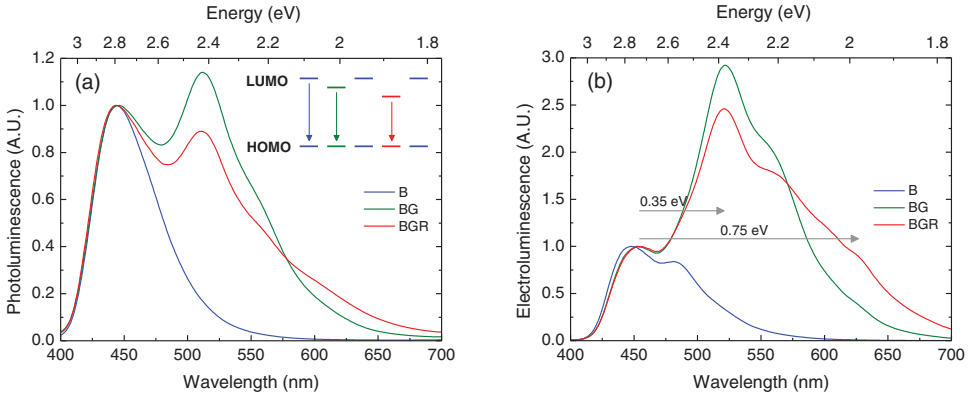

Figure 2. a) The photoluminescence spectra of B, BG, and BGR. The excitation was at the maximum of the absorption at 370 nm. The inset shows a schematic representation of the band diagram of the white-emitting copolymer. b) The electroluminescence of 90 nm PLEDs, driven at a bias of 5 V, normalized to the blue emission peak at 450 nm. The arrows indicate the energy offset between the blue emission peak and the green and red emission.

blue to green to red and from blue to red directly.[38] In the EL spectrum, the contribution from the green peak is much stronger and the red emission is better discernible. The concentrations of the dyes are too low for guest-to-guest transport to occur.[39,40] Consequently, the device current in the copolymer is carried by the blue backbone. Emission from the dyes can then originate from either recombination on the blue backbone and consecutive energy transfer to the dyes or from charge trapping and recombination on the dyes. Since the latter mechanism is not present in PL, the stronger contribution of the dyes in the EL spectrum can be attributed to charge trapping and recombination on the dyes. As a result, it can be expected that the electronic processes are dominant in determining the spectrum of the white-emitting diode. For white-emitting OLEDs containing a blend of dyes it has been concluded previously that emission due to trapping and recombination on dyes is dominant over energy transfer.[7,9,12,14,17,41–43] **Figure 3** shows the voltage dependence of the EL spectrum of a 90 nm white-emitting BGR PLED, normalized to the blue emission peak. A clear color shift is observed; with increasing bias the relative contribution of red decreases and the emission shifts towards blue. Our device

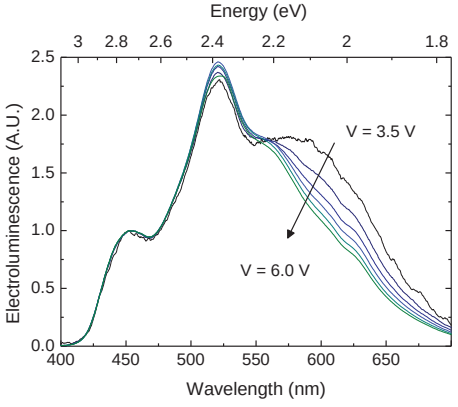

Figure 3. The voltage dependence of the electroluminescence spectrum of an 90 nm BGR PLED. The bias ranged from $V = 3.5$ V to $V = 6.0$ V and the intensity was normalized to the blue emission peak at 450 nm.

model enables us to quantify the voltage dependencies of the Langevin (blue) and SRH (red) recombination mechanisms and their role in the observed color shift.

2.1. Charge Transport

As a first step towards a quantitative description of a white-emitting PLED we analyze the electron and hole transport in the host and host-guest systems. In earlier work we have investigated the charge transport in the blue backbone material.[44] The hole transport could be described as trap-free with a hole mobility of $\mu_h \approx 1 \times 10^{-11}$ m^2 V^{-1} s^{-1}. The intrinsic mobility of the free electrons was found to be at least one order of magnitude larger than the hole mobility although the electron current was hampered by electron traps, assumed to be distributed exponentially in the bandgap. We have recently found that the electron transport in PPV derivatives can alternatively be described with a Gaussian distribution of electron traps,[27] which justifies a re-examination of the electron transport in the blue polymer. **Figure 4** shows the current–voltage (J–V) characteristics of electron-only devices of the blue-emitting polymer with three different thicknesses. A fit procedure was used to determine the optimal set of mobility parameters and trap parameters describing the electron transport in the blue backbone polymer. The thickness and temperature dependence of the electron transport could be described with a density-dependent mobility according to the EGDM with $\sigma = 0.09$ eV, $a = 0.93$ nm, and $\mu_0^* = 4.2 \times 10^{-8}$ m^2 V^{-1} s^{-1}, and a Gaussian trap located at 0.81 eV below the lowest unoccupied molecular orbital (LUMO) of the blue-emitting polymer with a trap density of $N_t = 1 \times 10^{23}$ m^{-3}. To limit the number of unknown parameters, the width of the Gaussian trap distribution was assumed to be equal to the width of the density of states (DOS) of the LUMO at $\sigma_t = 0.09$ eV. We note that especially at low bias, the quality of the fit is improved significantly by assuming a Gaussian trap density compared to an exponential trap density.

Since the green and red dyes by definition have a smaller bandgap than the blue backbone, they are expected to introduce charge traps for the transport through the blue backbone.

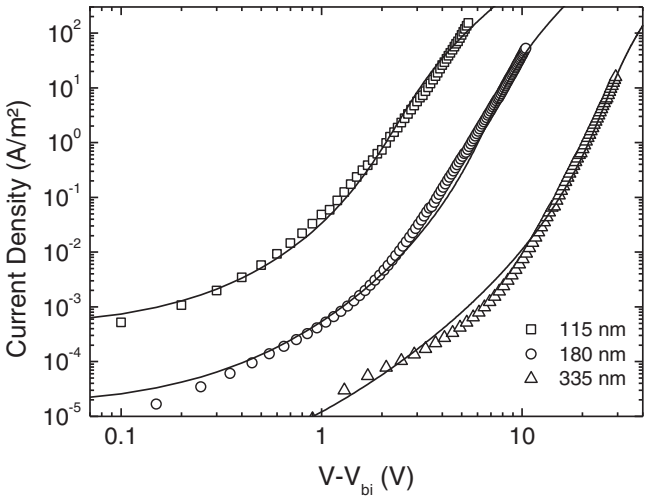

Figure 4. The room temperature electron transport of the blue backbone polymers. The lines are fits of the numerical device model, including a density-dependent mobility with parameters $\sigma = 0.09$ eV, $a = 0.93$ nm, $\mu_0^* = 4.2 \times 10^{-8}$ m^2 V^{-1} s^{-1} and a Gaussian trap distribution with parameters $E_t = 0.81$ eV, $\sigma_t = 0.09$ eV, and $N_t = 1 \times 10^{23}$ m^{-3}.

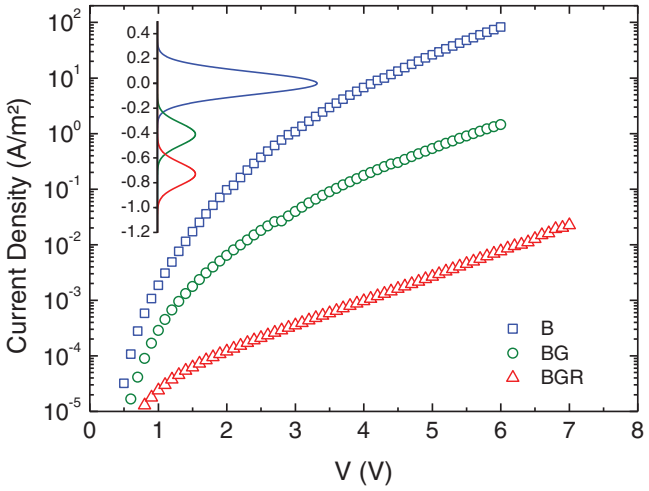

Figure 6. Electron transport of the three polymers investigated. The active layer thickness is 135 nm. The inset shows a schematic density of states of the LUMO and the green and red dyes. The concentrations of the dyes are exaggerated by a factor 1000.

Figure 5a shows *J*–*V* characteristics of 130 nm double carrier devices (PLEDs) of the three polymers. A clear decrease in device current is observed upon the inclusion of the dyes. The question now arises whether the dyes act as hole traps, electron traps, or perhaps as both. Figure 5b shows the *J*–*V* characteristics of hole-only diodes of the three polymers with a thickness of 130 nm. It is apparent that the hole transport is essentially unaffected by the inclusion of the dyes, which was also confirmed by time-of-flight measurements.[45] This demonstrates that the dyes do not act as hole traps and that the highest occupied molecular orbital (HOMO) levels of the dyes are thus located energetically at, or below, the HOMO level of the blue backbone. For recombination on the dyes to occur the hole can either originate directly from the blue backbone HOMO or via the dye HOMO level. The latter case would be improbable if the dye HOMO level would lie well below the host HOMO level. It can therefore be concluded that both the green and red dye are relatively well aligned with the HOMO level of the blue backbone material. From this result it can already be anticipated that the dyes should function as electron traps.

Figure 6 shows the *J*–*V* curves of 135 nm electron-only devices. Indeed, the incorporation of the green dye causes a dramatic decrease of the electron current. The inclusion of the red dye reduces the electron current even further. This clearly demonstrates that the dyes behave as electron traps for the electron transport through the blue backbone. Because the HOMO levels of the dyes and the blue backbone are well aligned, the energy offset between the LUMO levels from the blue backbone LUMO can be directly estimated from the emission spectrum (Figure 2). From this, we estimate the trap depths at ≈0.35 eV

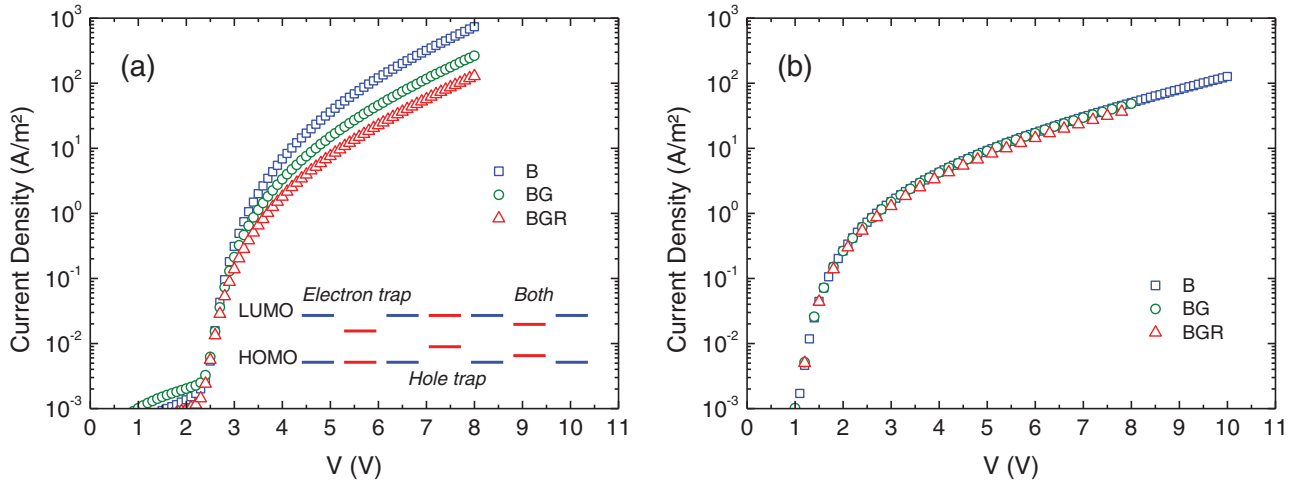

Figure 5. a) Device current of 130 nm PLEDs of B, BG, and BGR and b) device current of hole-only devices of 130 nm B, BG, and BGR devices. The inset of (a) shows a schematic representation of the possible alignments of the energy levels of the dyes with respect to the backbone material.

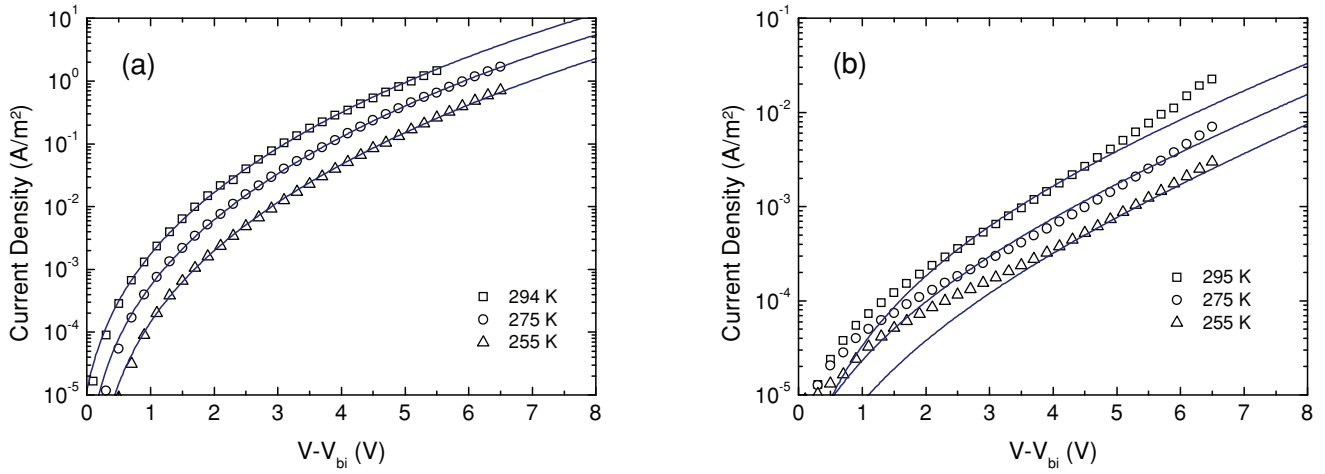

Figure 7. Temperature-dependent electron transport of the polymers a) BG and b) BGR measured in a 135 nm electron-only device. The lines are fits of the device model, including a Gaussian electron trap to represent the green and red dye.

and ≈0.75 eV for the green and red dyes, respectively. Furthermore, the density of the dyes may be roughly estimated from the feed ratio of the monomers during the syntheses of the polymers. Based on the assumption of a density of 1 g cm^{-3}, the densities of the green and red dye amounts to 1×10^{24} m^{-3} and 2×10^{23} m^{-3}, respectively.

Since the dye concentration is considerably below the percolation limit, the electron current is carried solely through the blue host polymer LUMO. It is therefore reasonable to assume the same mobility parameters as determined for the blue backbone polymer. To describe the temperature-dependent electron transport in the BG and BGR polymers (**Figure 7**) we incorporate Gaussian distributed electron traps representing the green and red dye. Again, the width of the trap distributions is assumed to be equal to the width of the LUMO DOS at $\sigma_t = 0.09$ eV. The only free parameters remaining are then the trap density N_t and the trap depth E_t. The temperature-dependent electron transport in the BG polymer (Figure 7a) can be accurately described using the parameter set E_t = 0.41 eV and $N_t = 3 \times 10^{23}$ m^{-3}. Although the fitted trap depth agrees very well with the estimated trap depth, the obtained trap density is lower than one might expect from the feed ratios. The reason for this discrepancy is yet unknown. One explanation would be that not all monomers involved in the synthesis are electrically active in the polymer. Finally, keeping all parameters fixed and including an additional trap distribution representing the red dye, the temperature-dependent electron current in the BGR polymer can be described (Figure 7b). For this case the quality of the fit that could be achieved is slightly less. We do not know the reason for this discrepancy. However, it should be noted that the electron currents as measured in the BGR electron-only devices are rather low, which makes it more sensitive to the influence of leakage currents or noise. The trap parameters found for the red dye are a trap depth of $E_t = 0.73$ eV and a trap density of $N_t = 3 \times 10^{23}$ m^{-3}. Both the trap depth and density are in good agreement to the expected values.

2.2. Device Modeling

At this point, all the ingredients for a complete device simulation of the white-emitting PLED have been determined. As mentioned above, the hole transport of the BGR polymer is equal to the hole transport of the blue backbone polymer. We can therefore adopt the hole transport parameters as obtained previously.[44] The electron transport can be described as the electron transport in the blue backbone material, with the inclusion of two additional electron trap distributions representing the green and red dye. The recombination rate of the blue light is then given by the Langevin equation, while the emission from the green and the red dye is calculated using the SRH relation. Note that the trap-assisted recombination for the electron traps that are already present in the blue backbone polymer is taken as non-radiative, similar to PPV-based PLEDs.[28] For the SRH recombination only the capture coefficients C_n and C_p remain as free parameters.

Figure 8 shows the room temperature *J–V* characteristics of BGR PLEDs with three different thicknesses of the active layer. Using a capture coefficient of $C_n = C_p = 5 \times 10^{-18}$ m^3 s^{-1} an excellent fit is obtained for the device current of the BGR PLED. This coefficient is slightly larger than the coefficient reported for poly(2-methoxy-5-(2′-ethylhexyloxy)-*p*-phenylene vinylene) (MEH-PPV) ($C_n = 9 \times 10^{-19}$ $m^3 s^{-1}$).[28] Having established a numerical description of the white-emitting PLED, we can use our device model to evaluate the spatial distribution of internal quantities such as the electron and hole density. Of direct relevance for the photon outcoupling efficiency is the position of the recombination zone. The spatially resolved recombination rate is calculated by the Langevin relation (Equation 1) for the blue emission, while the red emission is attributed to SRH recombination on the red dye (Equation 2). **Figure 9** shows the distribution of the recombination rate of blue and red in a 130 nm thick RGB PLED at biases of $V = 3$ V and $V = 8$ V. It was previously found that the blue backbone PLED changed from hole dominated to electron dominated with

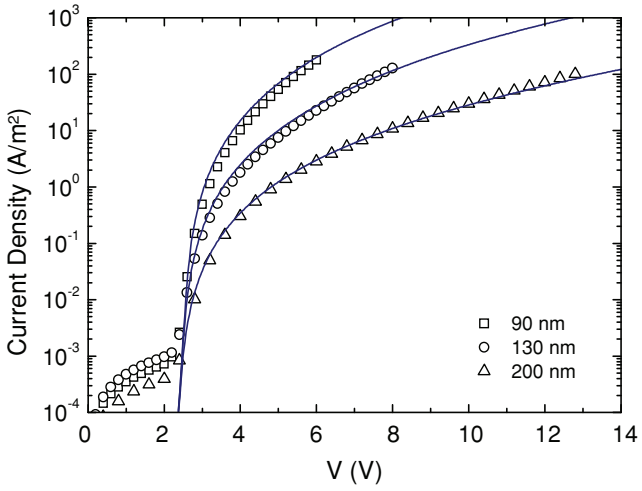

Figure 8. Device current of BGR PLED with three different thicknesses. The lines represent the fits of the device model.

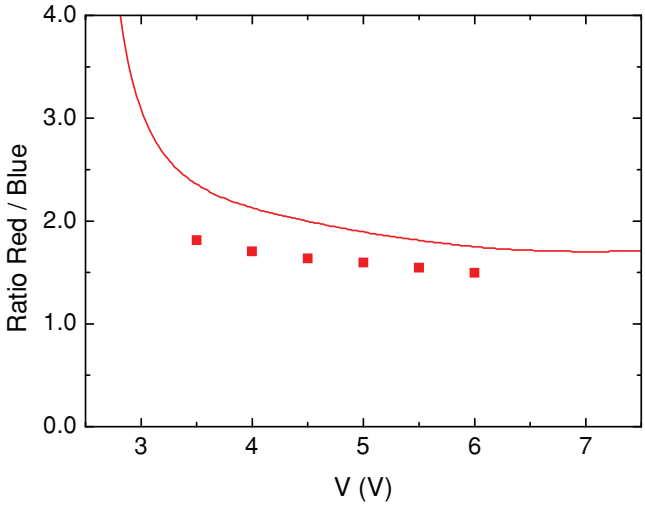

Figure 10. The ratio of red emission relative to the blue emission of a 90 nm BGR PLED, as obtained from the spectrum in Figure 3. The line is the calculated ratio of SRH recombination to Langevin recombination.

increasing bias, leading to a shift of the recombination zone.[44] In contrast, due to the electron trapping dyes, the white-emitting BGR PLED is hole dominated over the entire voltage range and the recombination zone is located close to the cathode. A recombination zone close to the cathode is disadvantageous for the device efficiency because a part of the formed exitons will be lost due to quenching by the metallic cathode.[46,47] As a result the performance of the materials system studied is strongly hindered by the unbalanced charge transport. For an optimized device, the recombination should lie in the middle of the emissive layer. It is therefore important to engineer the backbone and the dyes in such a way that, not only the output spectrum is observed as white, but also that the charge transport remains well balanced. This may be achieved by tuning the energy levels of the dyes and backbone polymer. For example, shifting the energy levels of the present host polymer down will reduce the electron trapping and will induce or enhance hole trapping.

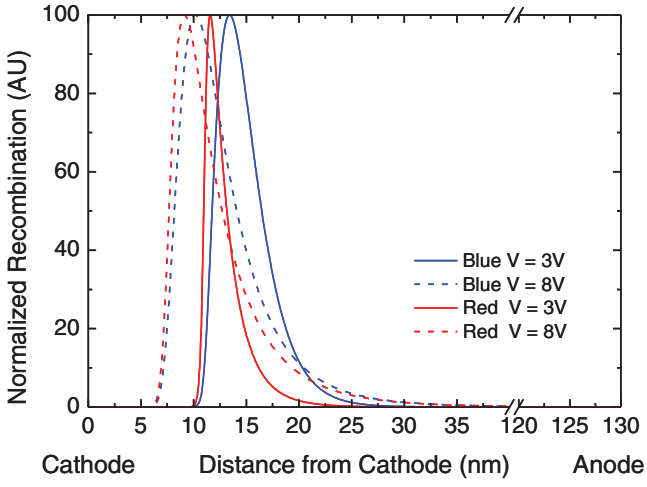

Figure 9. Distribution of the blue and red recombination in a 130 nm thick white-emitting PLED, for voltages of $V = 3$ V and $V = 8$ V.

As a final step, we examine the proportion of red emission relative to the blue emission. We extract the ratio red/blue from the EL spectra shown in Figure 3, defined as the intensity of the red emission at 575 nm divided by the intensity of the blue peak. The total blue and red emission is calculated as the integral of Langevin recombination (blue) and SRH recombination (red). Over the voltage range measured, the measured ratio red/blue decreases from ≈1.8 to ≈1.5. The numerically calculated ratio exhibits a similar decrease over that voltage range (**Figure 10**). We took into account that both Langevin and SRH recombination are simultaneously enhanced at high bias voltage due to a mobility increase.[48] Only an approximate fit is achieved, however it should be noted that there are several factors that inhibit a complete quantitative description of the output spectrum. First, it cannot be assumed that the blue backbone and the dyes have an equal luminescence efficiency. As a result, the calculated recombination rate cannot be directly translated into the emission intensity. Second, the contribution of energy transfer from the blue backbone to the red dye is not taken into account in the model. However, assuming that the energy transfer is independent of the applied bias, the voltage dependence of the red/blue ratio is not influenced by energy transfer. Finally, for a similar copolymer it was found that the field dependence of exciton quenching also introduces a small voltage dependence of the spectrum.[15] Considering the many effects contributing to the emission spectrum of a PLED, we consider the result as shown in Figure 10 to be reasonably satisfactory. As can be observed in the EL spectra in Figure 3, the emission from the green dye (relative to the blue emission) exhibits a considerably weaker voltage dependence than the red emission. While the clearly different voltage dependencies of the red and blue emission point to different recombination mechanisms, the same cannot be claimed for the green emission. It would therefore be questionable to attribute the green emission solely to SRH recombination on the green dye. As a result, we cannot apply the same analysis to the green emission peak.

3. Conclusion

In conclusion, we have presented a complete electrical device description of a single-layer white-emitting PLED. All parameters involved in the description of the charge transport and recombination in the PLED, i.e., the mobility parameters and the trap parameters of the dyes, have been determined independently from single-carrier devices. By incorporating trap-assisted recombination the electrical characteristics can be consistently modeled and the recombination rates on the dyes and on the blue backbone can be calculated. The observed color shift of the white PLED can qualitatively be reproduced by the ratio of red to blue emission. Since a (fluorescent) red dye in a blue-emitting backbone is, by definition, expected to act as a charge trap, the competition of the two different recombination mechanisms is expected to be a general behavior in single-layer white-emitting PLEDs. In the polymer studied here, the incorporation of SRH recombination for the red emission suffices to explain the shift of the emission spectrum. However, this does not exclude that a shift of the recombination zone may contribute to the color shift. In this work only a minor shift of the recombination zone was observed, so that the optical effects of a shift of the recombination zone are not significant for the emission spectrum.

4. Experimental Section

PLEDs and hole-only devices were fabricated on glass substrates with a patterned indium tin oxide layer. The substrates are ultrasonically cleaned and treated with UV-ozone. A layer of poly(3,4-ethylene dioxythiophene):poly(styrene sulfonate) (PEDOT:PSS) (Clevios P VP Al 4083, supplied by H.C. Starck) was spin-coated from solution and baked (140 °C). The polymer layers were spin-coated in a nitrogen atmosphere from a toluene solution. For the PLEDs and electron-only devices, the cathodes consisted of a Ba layer (5 nm) and an Al capping layer (100 nm) and were deposited by thermal evaporation (chamber pressure $\approx 10^{-6}$ mbar). For hole-only devices, the cathode consisted of a Pd layer (20 nm) capped with an Au layer (80 nm). Electron-only devices were fabricated on glass substrates with an Al bottom contact (30 nm) functioning as the anode. No electroluminescence was observed for the single carrier devices, which confirms the unipolar transport. The devices were characterized in a nitrogen atmosphere using a computer controlled Keithley 2400 SourceMeter. Emission spectra measurements where performed with an Ocean Optics USB2000 spectrometer.

Acknowledgements

The authors thank the European Commission for funding this work under contract IST-004607 (OLLA). The authors acknowledge Merck KGaA for the supply of the polymer. This article was amended on May 23, 2012 to correct an error in Figure 10 that was present in the version originally published online.

Received: November 9, 2011
Revised: January 11, 2012
Published online: February 23, 2012

[1] C. W. Tang, S. A. VanSlyke, *Appl. Phys. Lett.* **1987**, *51*, 913.
[2] J. Kido, M. Kimura, K. Nagai, *Science* **1995**, *267*, 1332.
[3] P. E. Burrows, S. R. Forrest, S. P. Sibley, M. E. Thompson, *Appl. Phys. Lett.* **1996**, *69*, 2959.
[4] R. S. Deshpande, V. Bulovic, S. R. Forrest, *Appl. Phys. Lett.* **1999**, *75*, 888.
[5] M. Berggren, O. Inganäs, G. Gustafsson, J. Rasmusson, M. R. Andersson, T. Hjertberg, O. Wennerström, *Nature* **1994**, *372*, 444.
[6] J. Kido, H. Shionoya, K. Nagai, *Appl. Phys. Lett.* **1995**, *67*, 2281.
[7] H. Suzuki, S. Hoshino, *J. Appl. Phys.* **1996**, *79*, 8816.
[8] M. Granström, O. Inganäs, *Appl. Phys. Lett.* **1996**, *68*, 147.
[9] S. Tasch, E. J. W. List, O. Ekstrom, W. Graupner, G. Leising, P. Schlichting, U. Rohr, Y. Geerts, U. Scherf, K. Mullen, *Appl. Phys. Lett.* **1997**, *71*, 2883.
[10] C. Ego, D. Marsitzky, S. Becker, J. Zhang, A. C. Grimsdale, K. Müllen, J. D. MacKenzie, C. Silva, R. H. Friend, *J. Am. Chem. Soc.* **2011**, *125*, 437.
[11] G. Tu, Q. Zhou, Y. Cheng, L. Wang, D. Ma, X. Jing, F. Wang, *Appl. Phys. Lett.* **2004**, *85*, 2172.
[12] W. Wu, M. Inbasekaran, M. Hudack, D. Welsh, W. Yu, Y. Cheng, C. Wang, S. Kram, M. Tacey, M. Bernius, R. Fletcher, K. Kiszka, S. Munger, J. O'Brien, *Microelectron. J.* **2004**, *35*, 343.
[13] J. Liu, Z. Y. Xie, Y. X. Cheng, Y. H. Geng, L. X. Wang, X. B. Jing, F. S. Wang, *Adv. Mater.* **2007**, *19*, 531.
[14] J. Liu, L. Chen, S. Y. Shao, Z. Y. Xie, Y. X. Cheng, Y. H. Geng, L. X. Wang, X. B. Jing, F. S. Wang, *Adv. Mater.* **2007**, *19*, 4224.
[15] M. de Kok, W. Sarfert, R. Paetzold, *Thin Solid Films* **2010**, *518*, 5265.
[16] Y. W. Ko, C. H. Chung, J. H. Lee, Y. H. Kim, C. Y. Sohn, B. C. Kim, C. S. Hwang, Y. H. Song, J. Lim, Y. J. Ahn, G. W. Kang, N. Lee, C. Lee, *Thin Solid Films* **2003**, *426*, 246.
[17] M. Suzuki, T. Hatakeyama, S. Tokito, F. Sato, *IEEE J. Sel. Top. Quantum Electron.* **2004**, *10*, 115.
[18] B. Hu, F. E. Karasz, *J. Appl. Phys.* **2003**, *93*, 1995.
[19] J. Huang, G. Li, E. Wu, Q. Xu, Y. Yang, *Adv. Mater.* **2006**, *18*, 114.
[20] Y. S. Wu, S. W. Hwang, H. H. Chen, M. T. Lee, W. J. Shen, C. H. Chen, *Thin Solid Films* **2005**, *488*, 265.
[21] M. C. Gather, R. Alle, H. Becker, K. Meerholz, *Adv. Mater.* **2007**, *19*, 4460.
[22] M. P. Langevin, *Ann. Chim. Phys.* **1903**, *28*, 433.
[23] U. Albrecht, H. Bässler, *Phys. Status Solidi B* **1995**, *191*, 455.
[24] P. W. M. Blom, M. J. M. de Jong, S. Breedijk, *Appl. Phys. Lett.* **1997**, *71*, 930.
[25] P. W. M. Blom, M. J. M. de Jong, J. J. M. Vleggaar, *Appl. Phys. Lett.* **1996**, *68*, 3308.
[26] M. M. Mandoc, B. de Boer, G. Paasch, P. W. M. Blom, *Phys. Rev. B* **2007**, *75*, 193202.
[27] H. T. Nicolai, M. M. Mandoc, P. W. M. Blom, *Phys. Rev. B* **2011**, *83*, 195204.
[28] M. Kuik, H. T. Nicolai, M. Lenes, G. A. H. Wetzelaer, M. Lu, P. W. M. Blom, *Appl. Phys. Lett.* **2011**, *98*, 093301.
[29] W. Shockley, W. T. Read, *Phys. Rev.* **1952**, *87*, 835.
[30] R. N. Hall, *Phys. Rev.* **1952**, *87*, 387.
[31] C. T. Sah, R. N. Noyce, W. Shockley, *Proc. IRE* **1957**, *45*, 1228.
[32] G. A. H. Wetzelaer, M. Kuik, H. T. Nicolai, P. W. M. Blom, *Phys. Rev. B* **2011**, *83*, 165204.
[33] L. J. A. Koster, E. C. P. Smits, V. D. Mihailetchi, P. W. M. Blom, *Phys. Rev. B* **2005**, *72*, 085205.
[34] C. Tanase, E. J. Meijer, P. W. M. Blom, D. M. de Leeuw, *Phys. Rev. Lett.* **2003**, *91*, 216601.
[35] W. F. Pasveer, J. Cottaar, C. Tanase, R. Coehoorn, P. A. Bobbert, P. W. M. Blom, D. M. de Leeuw, M. A. J. Michels, *Phys. Rev. Lett.* **2005**, *94*, 206601.
[36] D. Buchhauser, M. Scheffel, W. Rogler, C. Tschamber, K. Heuser, A. Hunze, G. Gieres, D. Henseler, W. Jakowetz, K. Diekmann, A. Winnacker, H. Becker, A. Büsing, A. Falcou, L. Rau, S. Vögele, S. Göttling, *Proc. SPIE-Int. Soc. Opt. Eng.* **2004**, *5519*, 70.
[37] A. Falcou, A. Büsing, S. Heun, J. Steiger, A. Gerhard, N. Schulte, H. Becker, WO Patent 05/030827 (2005).

[38] M. Anni, S. Lattante, M. M. De Kok, R. Cingolani, G. Gigli, *Appl. Phys. Lett.* **2006**, *89*, 221903.
[39] Y. Y. Yimer, P. A. Bobbert, R. Coehoorn, *J. Phys.: Condens. Matter* **2008**, *20*, 335204.
[40] H. T. Nicolai, A. J. Hof, M. Lu, P. W. M. Blom, R. J. de Vries, R. Coehoorn, *Appl. Phys. Lett.* **2011**, *99*, 203303.
[41] S. E. Shaheen, B. Kippelen, N. Peyghambarian, J. F. Wang, J. D. Anderson, E. A. Mash, P. A. Lee, N. R. Armstrong, Y. Kawabe, *J. Appl. Phys.* **1999**, *85*, 7939.
[42] P. A. Lane, L. C. Palilis, D. F. O'Brien, C. Giebeler, A. J. Cadby, D. G. Lidzey, A. J. Campbell, W. Blau, D. D. C. Bradley, *Phys. Rev. B* **2001**, *63*, 235206.
[43] X. Gong, M. R. Robinson, J. C. Ostrowski, D. Moses, G. C. Bazan, A. J. Heeger, *Adv. Mater.* **2002**, *14*, 581.
[44] H. T. Nicolai, A. Hof, J. L. M. Oosthoek, P. W. M. Blom, *Adv. Funct. Mater.* **2011**, *21*, 1505.
[45] M. A. Parshin, J. Ollevier, M. Van der Auweraer, M. M. de Kok, H. T. Nicolai, A. J. Hof, P. W. M. Blom, *J. Appl. Phys.* **2008**, *103*, 113711.
[46] H. Becker, S. E. Burns, R. H. Friend, *Phys. Rev. B* **1997**, *56*, 1893.
[47] D. E. Markov, P. W. M. Blom, *Appl. Phys. Lett.* **2005**, *87*, 233511.
[48] M. Kuik, L. J. A. Koster, G. A. H. Wetzelaer, P. W. M. Blom, *Phys. Rev. Lett.* **2011**, *107*, 256805.